

Optimal design of a class of generalized symmetric Gough–Stewart parallel manipulators with dynamic isotropy and singularity-free workspace

Zhizhong Tong^{†*}, Jingfeng He[†], Hongzhou Jiang[†] and Guangren Duan[‡]

[†]*School of Mechatronics Engineering, Harbin Institute of Technology, Harbin 150001, P. R. China*

[‡]*School of Astronautics, Harbin Institute of Technology, Harbin 150001, P. R. China*

(Received in Final Form: May 11, 2011; accepted May 9, 2011. First published online: June 23, 2011)

SUMMARY

In this paper, the definition of generalized symmetric Gough–Stewart parallel manipulators is presented. The concept of dynamic isotropy is proposed and the singular values of the bandwidth matrix are introduced to evaluate dynamic isotropy and solved analytically. Considering the payload's mass-geometry characteristics, the formulations for completely dynamic isotropy are derived in close form. It is proven that a generalized symmetric Gough–Stewart parallel manipulator is easier to achieve dynamic isotropy and applicable in engineering applications. An optimization procedure based on particle swarm optimization is proposed to obtain better dexterity and large singularity-free workspace, which guarantees the optimal solution and gives mechanically feasible realization.

KEYWORDS: Parallel manipulators; Generalized symmetric Gough–Stewart; Dynamic isotropy; Optimal design; PSO.

1. Introduction

Gough–Stewart parallel manipulators have been employed in a wide variety of areas, such as manipulation, matching, control, tracking, and haptic force feedback. However, due to highly nonlinear, highly time-varying, and highly dynamic coupling, it is hardly to realize precision pointing, motion planning, control scheme, calibration, and compensation, especially in many high-precision applications, including laser weapon pointing, scanning microscopes, and integrated circuit fabrication. In general, decoupled and isotropic measure is usually considered as one of the desired performance. Designing a parallel robot that is isotropic in one pose or over its full workspace is often considered as a design objective.¹ Isotropic manipulators are also generally considered as designs with optimum dexterity.²

Isotropy can be categorized into kinematic isotropy, static isotropy, and dynamic isotropy. Kinematic isotropy implies the ability of the manipulator end-effector to move equally well in all spatial directions, while static isotropy

concerns the ability of resisting forces and moments. In the past research, kinematic isotropy and static isotropy have been studied in-depth.^{3–6} The algebraic formulations were derived by symbolic computations and obtained a family of configurations in closed form,^{5–6} but it is a little difficult to deduce the formulation, owing to the complexity of the structure, and the limitation of calculation methods. Orthogonal performance implies that a Gough–Stewart parallel manipulator is decoupled. McInroy *et al.* explored various properties of the Jacobian in order to achieve the optimum design of orthogonal Gough–Stewart parallel manipulators.^{7–12} Jafari *et al.* proposed an analytical description of the set of all such manipulators and developed a method allowing the choice of optimal geometries among all the possible geometries.⁸ Yi *et al.* presented a novel method for generating classes of orthogonal Gough–Stewart parallel manipulators with an even number of struts.^{9–11} Their method gives more flexibility and still achieves isotropic manipulators. However, it is not easy to solve for the complete set of solutions in their work. Tsai *et al.* have got a large number of isotropy generators by solving the nonlinear equations analytically.¹² They have proposed optimal design methods and developed 6-DOF fully symmetric parallel manipulators or redundant manipulators with different shapes or different types of kinematic chains.^{13–15} However, a natural length scale during the kinematic isotropy or static isotropy design is lack due to the fact that the Jacobian elements are not dimensionally homogenous, and some researchers have tried to overcome this problem using length scales.^{16–17} It does limit the applications some.

In the previous work, they assumed that the motion reference point coincides with the geometric center of the movable platform or the mass-center of the payload, i.e., they did not consider the mass-center's influence and the mathematical description was omitted discovering the relationships between geometry of the manipulator, mass-center, and inertia parameters of the payload. McInroy *et al.* found several geometries and gave examples of three kinds of the mass-center distribution when obtaining an isotropic configuration.⁷ How to hunt and design an optimal manipulator for a given payload or special mass-center requirement? Does it exist that an analytical expression

* Corresponding author. E-mail: tongzhizhong@yahoo.com.cn

can describe the relationships between geometry of the manipulator and mass-center of the payload? What is more, the structure can be optimized with desired performances in the previous work. However, we prefer to focus on the dynamic response of a parallel manipulator in real applications. Theoretically, kinematic isotropy and static isotropy both have relations to geometry of the manipulator and stiffness of the struts. Unfortunately, these two performance measures cannot be used to evaluate the response of control system. The relative design routine is discrete from the view of practice. The designs of the structure optimum and the control system should be integrated rather than they are departed from each other. A new measure should be introduced to bridge the gap.

When a standard Gough–Stewart parallel manipulator is expected to achieve complete isotropy, the strictly physical restriction for the payload exists: $I_{ZZ} = 4I_{XX} = 4I_{YY}$.^{18–19} In practice, it is hardly to be satisfied for a real payload. Even if studied in single degree of freedom in the laboratory, it may require laborious work and tedious procedures as reported in literature.¹⁹ Could this restriction be loosen or broken down so that the real payload is valid and the manipulator is mechanical feasible?

In this paper, we will propose the concept of dynamic isotropy and derive the analytical formulations for complete dynamic isotropy to generate a class of the generalized symmetric parallel manipulators. Factually, the analytical algorithm does not guarantee the optimal solution or give possible realization. We will present a systematical design procedure based on particle swarm optimization (PSO) to obtain better dexterity, large singularity-free workspace, and without interactions among elements. Compared to the previous work, our optimal design procedure is based on the derived formulations and is not a purely numerical solution.

2. Dynamic Isotropy Measures

2.1. Architecture description

To solve the problems and testify our ideas, we focus on a more generalized class of Gough–Stewart parallel manipulators. For completeness, we give the following definition.

Definition 1: A parallel manipulator consists of a movable platform, a fixed base, and six struts, each with a linear actuator. The struts are partitioned into two groups: the first group with strut 1, 3, 5 and the second group with strut 2, 4, 6. The attached points of each strut are uniformly spaced on the circumferences of two circles on the movable platform and the fixed base, respectively. The three struts in each group are rotational symmetry and repeat every 120°. The parallel manipulators with this kind of configurations are defined as generalized symmetric Gough–Stewart parallel manipulators (GSGSPMs).

The architecture of a GSGSPM is shown in Fig. 1. It can be described by nine parameters at neutral position: $r_{a1}, r_{a2}, r_{b1}, r_{b2}, H, \alpha_1, \alpha_2, \beta_1,$ and β_2 . r_{a1} and r_{b1} denote the outer radii of the circles of the group with 1, 3, 5 of the movable platform and the fixed base, respectively. r_{a2} and r_{b2} denote the outer radii of the circles of the group with 2, 4, 6 of the movable

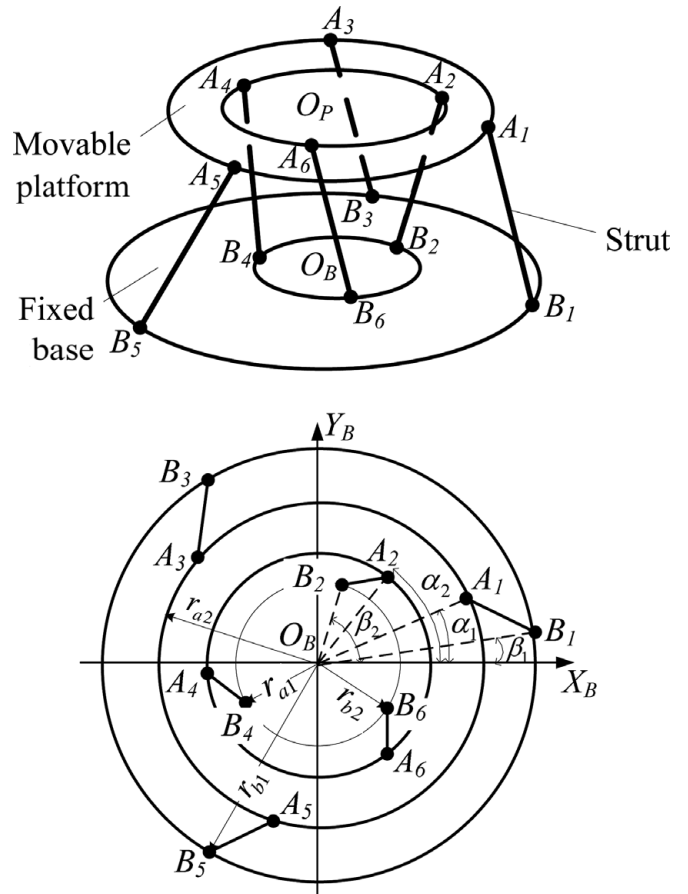


Fig. 1. The architecture and coordinate definition of a GSGSPM.

platform and the fixed base, respectively. The angles between the adjacent joint points of the strut 1, 2 and the X-axis are represented by $\alpha_1, \alpha_2, \beta_1,$ and β_2 . H denotes the height of GSGSPMs at neutral position. When $r_{a1} = r_{a2}, r_{b1} = r_{b2}, L_1 = L_2,$ and $\alpha_2 - \beta_2 = -(\alpha_1 - \beta_1)$, the manipulator satisfies mirror symmetry and belongs to a standard Gough–Stewart parallel manipulator.

According to the definition, two circles of each group are restricted in a common planar surface. In ref. [13], Tsai *et al.* studied the more general case in which four circles cannot be coplanar. The coplanar configuration is more mechanically feasible in practical applications. Therefore, the definition has fewer limitations, while it is approved in real areas.

With reference to Fig. 1, the body frame $\{P\}$ with origin O_P and the inertial frame $\{B\}$ with origin O_B are embedded in the movable platform and the fixed base, respectively. Let ${}^B_P\mathbf{R}$ denote the rotation matrix of the body frame $\{P\}$ relative to the inertial frame $\{B\}$. Denoting the upper joint points by ${}^P\mathbf{A}$ in frame $\{P\}$ and the lower joint points by ${}^B\mathbf{B}$ in frame $\{B\}$, the inverse Jacobian matrix \mathbf{J}^{-1} can be constructed directly by the unit vectors along struts. In this paper, the inverse Jacobian is considered to be of full rank. Otherwise, some constraints should be enforced to maintain kinematic stability. If the motion reference point of the platform does not coincide with the mass-center of the payload, the inverse Jacobian matrix \mathbf{J}^{-1} should be

written as

$$\mathbf{J}^{-1} = \begin{bmatrix} \mathbf{e}_1^T (\mathbf{B}^P \mathbf{R}^P \mathbf{A}_1 - \mathbf{P} \rho_c) \times \mathbf{e}_1 \\ \mathbf{e}_2^T (\mathbf{B}^P \mathbf{R}^P \mathbf{A}_2 - \mathbf{P} \rho_c) \times \mathbf{e}_2 \\ \mathbf{e}_3^T (\mathbf{B}^P \mathbf{R}^P \mathbf{A}_3 - \mathbf{P} \rho_c) \times \mathbf{e}_3 \\ \mathbf{e}_4^T (\mathbf{B}^P \mathbf{R}^P \mathbf{A}_4 - \mathbf{P} \rho_c) \times \mathbf{e}_4 \\ \mathbf{e}_5^T (\mathbf{B}^P \mathbf{R}^P \mathbf{A}_5 - \mathbf{P} \rho_c) \times \mathbf{e}_5 \\ \mathbf{e}_6^T (\mathbf{B}^P \mathbf{R}^P \mathbf{A}_6 - \mathbf{P} \rho_c) \times \mathbf{e}_6 \end{bmatrix}^T, \quad (1)$$

where the mass-center vector relative to the motion reference point is denoted by ρ_c in frame $\{B\}$ and ${}^P\rho_c$ in frame $\{P\}$ with $\rho_c = {}^B_P \mathbf{R}^P \rho_c + \mathbf{C}_p$, ${}^P\rho_c = [P_x \ P_y \ P_z]^T$. \mathbf{C}_p is the motion reference point with $\mathbf{C}_p = [0 \ 0 \ H]^T$. \mathbf{e}_i denotes the unit vector in direction of the i th actuator, which can be described by

$$\mathbf{e}_i = ({}^B_P \mathbf{R}^P \mathbf{A}_i + \mathbf{C}_p - {}^B \mathbf{B}_i) / L_i, \quad (2)$$

where L_i is the length of the i th strut.

Considering that a GSGSPM is symmetric with two rotational strut groups, a relationship must exist between the length of the strut 1 and the one of the strut 2, denoted by $\rho L_1 = L_2$. The configurations can be placed into two categories including the family that all strut lengths are equal if $\rho = 1$ and another family that they are alternate equal. The kinematic constraint $\rho L_1 = L_2$ by no means reflects any limitation the above deduced formulations, instead that it only affect the complexity of the problem. Of course, this is in spite of extensive searches using various methods.

2.2. Concept of dynamic isotropy

In this paper, we assume that the movable platform and the fixed base are rigid bodies. Using an elastic model for the variations of the joint variables as functions of the forces applied to the strut,²¹ the stiffness matrix \mathbf{K} of a GSGSPM in task space can be described by

$$\mathbf{K} = k_h \mathbf{J}^{-T} \mathbf{J}^{-1}, \quad (3)$$

where k_h is the elastic stiffness of the strut.

In many application fields, the mass and inertia of the movable platform are preponderant compared with the mass and inertia of the struts. The frame can be also selected to coincide with the orientation of the principle axes of the payload. Let \mathbf{M}_t denote the mass-inertia matrix of the payload, then \mathbf{M}_t should be diagonal. Multiplying Eq. (3) by the inverse mass-inertia matrix \mathbf{M}_t^{-1} results into

$$\mathbf{M}_t^{-1} \mathbf{K} = \begin{bmatrix} \frac{1}{m} \mathbf{I}_{3 \times 3} & 0 \\ 0 & \mathbf{I}_c^{-1} \end{bmatrix} k_h \mathbf{J}^{-T} \mathbf{J}^{-1}, \quad (4)$$

where $\mathbf{I}_{3 \times 3}$ is an identity matrix. m denotes the translational inertia mass. \mathbf{I}_c is the rotational mass-inertia matrix expressed in frame $\{B\}$, $\mathbf{I}_c = \text{diag}(I_{xx} \ I_{yy} \ I_{zz})$.

In fact, the stiffness of the struts conditions the manipulator’s stiffness. $\mathbf{M}_t^{-1} \mathbf{K}$ implies the natural

frequencies in task space. To evaluate the dynamic characteristics, we present a new definition.

Generally, square roots of the eigenvalues of Eq. (4) represent the natural frequency in task space.

Definition 2: $\mathbf{M}_t^{-1} \mathbf{K}$ describes the frequency coupling of different degrees of freedom of a GSGSPM. From the view of the control in practice, if k_h is not the elastic stiffness of the strut but the real stiffness of the close-loop control of the strut, $\mathbf{M}_t^{-1} \mathbf{K}$ implies the bandwidth or response performance. Thus, $\mathbf{M}_t^{-1} \mathbf{K}$ can be defined as the bandwidth matrix, denoted by \mathbf{F}_{bw} . If \mathbf{F}_{bw} is a scaling identity matrix, then a GSGSPM is orthogonal and isotropic and \mathbf{F}_{bw} is said to be defined as dynamic isotropy.

It is feasible to design a GSGSPM so that bandwidths of the struts are partially or fully equal by choosing an appropriate mechanical structure or by some control strategies, at least for some poses. The dynamic isotropy considers the mass geometry characteristics, different from the previous researches. The dynamic isotropy is valuable for practical applications and possibly bridges a gap in the structure optimization and the control system design.

2.3. Dynamic isotropy indices and measures

Bhattacharya uses the average of the minimal eigenvalue to qualify the stiffness of a robot over a given workspace.²⁰ In this paper, the singular values of the bandwidth matrix \mathbf{F}_{bw} , denoted by λ , are used as indices to evaluate the dynamic isotropy. Considering that GSGSPMs applied in many fields, such as flight simulation, force/torque sensor, and micro manipulator, often work at about neutral position, so local measures are used to evaluate dynamic isotropy.

The minimal singular value is a bottleneck to limit the performance of control system, so the first measure should be larger than a specified value

$$\eta_1 = \sigma_{\min} = \min\{\lambda\}. \quad (5)$$

Additionally, in order to ensure the uniformity of the bandwidth, we propose another measure for dynamic isotropy as

$$\eta_2 = \sqrt{\frac{\sigma_{\max}}{\sigma_{\min}}} = \sqrt{\frac{\max\{\lambda\}}{\min\{\lambda\}}}. \quad (6)$$

3. Analytical Formulation of Dynamic Isotropy

3.1. Symbolic expression of the bandwidth matrix and orthogonal conditions

The mass distribution of the payload is symmetrically at X – O – Y plane when the principle inertia axes are adjusted to coincide with X -axis and Y -axis of the frame without any bias, then ${}^P\rho_c = [0 \ 0 \ P_z]^T$. Simply extending and summarizing Eq. (4), \mathbf{F}_{bw} can be written in forms of $\mathbf{F}_{bw} = \begin{bmatrix} \mathbf{A}_{3 \times 3} & \frac{1}{m} \mathbf{C}_{3 \times 3} \\ \mathbf{I}_c^{-1} \mathbf{C}_{3 \times 3} & \mathbf{B}_{3 \times 3} \end{bmatrix}$. The submatrix $\mathbf{A}_{3 \times 3}$ is

$$\mathbf{A}_{3 \times 3} = \sum_{i=1}^6 \mathbf{e}_i \mathbf{e}_i^T. \quad (7)$$

Notice that $\mathbf{e}_1\mathbf{e}_1^T$ and $\mathbf{e}_2\mathbf{e}_2^T$ are both symmetric, then they are both diagonal. Therefore, $\mathbf{A}_{3 \times 3}$ is a symmetric matrix. Similarly, the submatrices satisfy

$$\mathbf{A}_{3 \times 3} = \begin{bmatrix} \Lambda_1 & 0 & 0 \\ 0 & \Lambda_1 & 0 \\ 0 & 0 & \Lambda_3 \end{bmatrix}, \quad \mathbf{B}_{3 \times 3} = \begin{bmatrix} \Lambda_4 & 0 & 0 \\ 0 & \Lambda_5 & 0 \\ 0 & 0 & \Lambda_6 \end{bmatrix},$$

$$\mathbf{C}_{3 \times 3} = \begin{bmatrix} C_{11} & -C_{12} & 0 \\ C_{12} & C_{11} & 0 \\ 0 & 0 & -C_{33} \end{bmatrix}, \tag{8}$$

where

$$\Lambda_1 = \frac{3k_h}{2mL_1^2L_2^2} (L_2^2(L_1^2 - H^2) + L_1^2(L_2^2 - H^2)),$$

$$\Lambda_2 = \Lambda_1 = \frac{3k_h}{2mL_1^2L_2^2} (L_2^2(L_1^2 - H^2) + L_1^2(L_2^2 - H^2)),$$

$$\Lambda_3 = \frac{3k_h H^2}{mL_1^2L_2^2} (L_1^2 + L_2^2),$$

$$\Lambda_4 = \frac{3k_h}{2I_{xx}L_1^2L_2^2} (H^2r_{b1}^2L_2^2 + H^2r_{b2}^2L_1^2 + \Delta_1(P_z - H)^2 + 2\Delta_2(P_z - H)),$$

$$\Lambda_5 = \frac{3k_h}{2I_{yy}L_1^2L_2^2} (H^2r_{b1}^2L_2^2 + H^2r_{b2}^2L_1^2 + \Delta_1(P_z - H)^2 + 2\Delta_2(P_z - H)),$$

$$\Lambda_6 = \frac{3k_h}{I_{zz}L_1^2L_2^2} (L_2^2r_{a1}^2r_{b1}^2 \sin^2(\alpha_1 - \beta_1) + L_1^2r_{a2}^2r_{b2}^2 \sin^2(\alpha_2 - \beta_2)),$$

$$C_{11} = \frac{3k_h H}{2L_1^2L_2^2} \Delta_3,$$

$$C_{12} = \frac{3k_h}{2L_1^2L_2^2} (\Delta_1(P_z - H) + \Delta_2),$$

$$C_{33} = \frac{3k_h H}{L_1^2L_2^2} \Delta_3,$$

$$\Delta_1 = L_2^2(L_1^2 - H^2) + L_1^2(L_2^2 - H^2),$$

$$\Delta_2 = -L_2^2 H r_{b1} (r_{b1} - r_{a1} \cos(\alpha_1 - \beta_1)) - L_1^2 H r_{b2} (r_{b2} - r_{a2} \cos(\alpha_2 - \beta_2)),$$

$$\Delta_3 = -(L_2^2 r_{a1} r_{b1} \sin(\alpha_1 - \beta_1) + L_1^2 r_{a2} r_{b2} \sin(\alpha_2 - \beta_2)).$$

In linear algebra, a matrix is symmetric, if and only if, it has an orthonormal basis of eigenvectors. It must have an only real orthogonal matrix \mathbf{P} , consisting of the orthonormal basis of eigenvectors such that $\mathbf{P}^{-1}\mathbf{K}\mathbf{P}$ is a diagonal matrix. A diagonal matrix multiplied by a diagonal matrix is also a diagonal matrix, so $\mathbf{M}_T^{-1}\mathbf{P}^{-1}\mathbf{K}\mathbf{P} = \mathbf{P}^{-1}\mathbf{F}_{bw}\mathbf{P} = \text{diag}(\lambda_1, \lambda_2, \lambda_3, \lambda_4, \lambda_5, \lambda_6)$. It implies that the translational and rotational motions of the manipulator are decoupled. Consequently, we obtain the following theorem.

Theorem 1: The diagonal matrix constructed by the primary diagonal elements of \mathbf{F}_{bw} is a unique characteristic matrix of the decoupled manipulator. The manipulator with this property is called an orthogonal GSGSPM.

According to this theorem, the sub matrix $\mathbf{C}_{3 \times 3}$ is a zero matrix. Two conditions must be met

$$\Delta_3 = -(L_2^2 r_{a1} r_{b1} \sin(\alpha_1 - \beta_1) + L_1^2 r_{a2} r_{b2} \sin(\alpha_2 - \beta_2)) = 0, \tag{9}$$

$$\Delta_1(P_z - H) + \Delta_2 = 0. \tag{10}$$

Factually, these two conditions are the kinematic orthogonal constraints. Rewriting Eqs. (9) and (10) yields

$$\sin(\alpha_1 - \beta_1) = -\frac{r_{a2}r_{b2}}{\rho^2 r_{a1}r_{b1}} \sin(\alpha_2 - \beta_2), \tag{11}$$

$$P_z^* = -\frac{\rho^2 r_{a1}(r_{a1} - r_{b1} \cos(\alpha_1 - \beta_1)) + r_{a2}(r_{a2} - r_{b2} \cos(\alpha_2 - \beta_2))}{\rho^2(L_1^2 - H^2) + (\rho^2 L_1^2 - H^2)} H. \tag{12}$$

With respect to Eq. (12), a compliance center exists consequentially for any GSGSPMs. At the compliance center, a GSGSPM is uncoupled. It may be useful for micromanipulators or parallel machine. If additional articulation attached on the manipulator, the inertia would be changed such that it is possible to make the manipulator orthogonal at a single configuration. Especially, the micromanipulator will have desired local performance due to quite small workspace.

3.2. Indices of dynamic isotropy

When a GSGSPM is orthogonal, the singular values of \mathbf{F}_{bw} can be derived directly as

$$\lambda_1^* = \sqrt{\Lambda_1} = \frac{\sqrt{3k_h}}{\sqrt{2m\rho}L_1} \sqrt{\rho^2(L_1^2 - H^2) + (\rho^2 L_1^2 - H^2)}, \tag{13}$$

$$\lambda_2^* = \sqrt{\Lambda_2} = \frac{\sqrt{3k_h}}{\sqrt{2m\rho}L_1} \sqrt{\rho^2(L_1^2 - H^2) + (\rho^2 L_1^2 - H^2)}, \tag{14}$$

$$\lambda_3^* = \sqrt{\Lambda_3} = \frac{\sqrt{3k_h}H}{\sqrt{m\rho}L_1} \sqrt{1 + \rho^2}, \tag{15}$$

$$\lambda_4^* = \sqrt{\Lambda_4} = \frac{\sqrt{3k_h}}{\sqrt{2I_{xx}}} \frac{H \sqrt{r_{a2}^2 r_{b1}^2 + r_{a1}^2 r_{b2}^2 - 2r_{a1} r_{b1} r_{a2} r_{b2} \cos((\alpha_1 - \beta_1) - (\alpha_2 - \beta_2))}}{L_1 \sqrt{\rho^2(L_1^2 - H^2) + (\rho^2 L_1^2 - H^2)}}, \tag{16}$$

$$\lambda_5^* = \sqrt{\Lambda_5} = \frac{\sqrt{3k_h}}{\sqrt{2I_{yy}}} \times \frac{H\sqrt{r_{a2}^2 r_{b1}^2 + r_{a1}^2 r_{b2}^2 - 2r_{a1} r_{b1} r_{a2} r_{b2} \cos((\alpha_1 - \beta_1) - (\alpha_2 - \beta_2))}}{L_1 \sqrt{\rho^2 (L_1^2 - H^2) + (\rho^2 L_1^2 - H^2)}} \quad (17)$$

$$\lambda_6^* = \sqrt{\Lambda_6} = \frac{\sqrt{3k_h}}{\sqrt{I_{zz} L_1 L_2}} \times \sqrt{L_2^2 r_{a1}^2 r_{b1}^2 \sin^2(\alpha_1 - \beta_1) + L_1^2 r_{a2}^2 r_{b2}^2 \sin^2(\alpha_2 - \beta_2)} = \frac{\sqrt{3k_h} r_{a1} r_{b1} |\sin(\alpha_1 - \beta_1)| \sqrt{1 + \rho^2}}{\sqrt{I_{zz} L_1}} \quad (18)$$

3.3. Conditions for complete isotropy

Since all the struts are arranged around two circles symmetrically, the translational manipulability in the X–Y direction is naturally isotropic, $\lambda_1^* = \lambda_2^*$. The rotational manipulability in the X–Y direction is isotropic only when $I_{xx} = I_{yy}$. For complete isotropy, the indices share a common value as below

$$\lambda_1^* = \lambda_2^* = \lambda_3^* = \lambda_4^* = \lambda_5^* = \lambda_6^* = \sqrt{2} \sqrt{\frac{k_h}{m}} \quad (19)$$

The height at neutral position, denoted by H_{ISO} , can be obtained from Eqs. (13) and (15)

$$H_{ISO} = \sqrt{\frac{2\rho^2}{3 + \rho^2} \sqrt{r_{a1}^2 + r_{b1}^2 - 2r_{a1} r_{b1} \cos(\alpha_1 - \beta_1)}} = \sqrt{\frac{2}{1 + 3\rho^2} \sqrt{r_{a2}^2 + r_{b2}^2 - 2r_{a2} r_{b2} \cos(\alpha_2 - \beta_2)}} \quad (20)$$

The compliance center can be given by

$$P_Z^* = -\frac{3 + \rho^2}{4\rho^2(1 + \rho^2)} \times \frac{\rho^2 r_{a1} (r_{a1} - r_{b1} \cos(\alpha_1 - \beta_1)) + r_{a2} (r_{a2} - r_{b2} \cos(\alpha_2 - \beta_2))}{(r_{a1}^2 + r_{b1}^2 - 2r_{a1} r_{b1} \cos(\alpha_1 - \beta_1))} H_{ISO}$$

or $P_Z^* = -\frac{\sqrt{2(3 + \rho^2)}}{4\rho(1 + \rho^2)} \times \frac{\rho^2 r_{a1} (r_{a1} - r_{b1} \cos(\alpha_1 - \beta_1)) + r_{a2} (r_{a2} - r_{b2} \cos(\alpha_2 - \beta_2))}{\sqrt{r_{a1}^2 + r_{b1}^2 - 2r_{a1} r_{b1} \cos(\alpha_1 - \beta_1)}} \quad (21)$

The complete isotropy condition can be summarized resulting from Eqs. (13) and (15) and Eqs. (16)

and (18).

$$\begin{cases} \frac{I_{zz}}{I_{xx}} = 4(1 + \rho^2)^2 \times \frac{r_{a1}^2 r_{b1}^2 \sin^2(\alpha_1 - \beta_1)}{r_{a2}^2 r_{b2}^2 + r_{a1}^2 r_{b2}^2 - 2r_{a1} r_{b1} r_{a2} r_{b2} \cos((\alpha_1 - \beta_1) - (\alpha_2 - \beta_2))}, \\ \frac{I_{zz}}{m} = \frac{3 + \rho^2}{2} \frac{r_{a1}^2 r_{b1}^2 \sin^2(\alpha_1 - \beta_1)}{r_{a1}^2 + r_{b1}^2 - 2r_{a1} r_{b1} \cos(\alpha_1 - \beta_1)}, \\ \frac{\rho^2 (r_{a1}^2 + r_{b1}^2 - 2r_{a1} r_{b1} \cos(\alpha_1 - \beta_1))}{3 + \rho^2} = \frac{r_{a2}^2 + r_{b2}^2 - 2r_{a2} r_{b2} \cos(\alpha_2 - \beta_2)}{1 + 3\rho^2}. \end{cases} \quad (22)$$

Let $p = \frac{r_{a1}}{r_{b1}}$, $q = \frac{r_{a2}}{r_{b2}}$, and $n = \frac{r_{a2}}{r_{a1}}$, then $\frac{q}{np} = \frac{r_{b1}}{r_{b2}}$. Substituting them in Eq. (21), we can obtain

$$\begin{cases} \frac{\sin(\alpha_1 - \beta_1)}{-\sin(\alpha_2 - \beta_2)} = \frac{n^2 p}{\rho^2 q} \quad \text{or} \quad \frac{p}{q} = \frac{\rho^2 \sin(\alpha_1 - \beta_1)}{-n^2 \sin(\alpha_2 - \beta_2)}, \\ P_Z^* = -\frac{\sqrt{2(3 + \rho^2)}}{4\rho(1 + \rho^2)} \times \frac{\rho^2 (p^2 - p \cos(\alpha_1 - \beta_1)) + (n^2 p^2 - n^2 \frac{p^2}{q} \cos(\alpha_2 - \beta_2))}{\sqrt{p^2 + 1 - 2p \cos(\alpha_1 - \beta_1)}} r_{b1}. \end{cases} \quad (23)$$

Similarly, Eq. (22) can be summarized as

$$\begin{cases} \frac{I_{zz}}{I_{xx}} = \frac{4(1 + \rho^2)^2}{n^2} \frac{\sin^2(\alpha_1 - \beta_1)}{1 + \left(\frac{p}{q}\right)^2 - 2\left(\frac{p}{q}\right) \cos((\alpha_1 - \beta_1) - (\alpha_2 - \beta_2))}, \\ \text{or} \quad \frac{I_{zz}}{I_{xx}} = \frac{4(1 + \rho^2)^2}{n^2} \times \frac{\sin^2(\alpha_1 - \beta_1)}{1 + \left(\frac{\rho^2 \sin(\alpha_1 - \beta_1)}{-n^2 \sin(\alpha_2 - \beta_2)}\right)^2 - 2\left(\frac{\rho^2 \sin(\alpha_1 - \beta_1)}{-n^2 \sin(\alpha_2 - \beta_2)}\right) \cos((\alpha_1 - \beta_1) - (\alpha_2 - \beta_2))}, \\ \frac{I_{zz}}{m} = \frac{3 + \rho^2}{2} \frac{p^2 \sin^2(\alpha_1 - \beta_1)}{p^2 + 1 - 2p \cos(\alpha_1 - \beta_1)} r_{b1}^2, \\ \frac{\rho^2 (p^2 + 1 - 2p \cos(\alpha_1 - \beta_1))}{3 + \rho^2} = \frac{n^2 p^2 + \frac{n^2 p^2}{q^2} - 2\frac{n^2 p^2}{q} p \cos(\alpha_2 - \beta_2)}{1 + 3\rho^2}. \end{cases} \quad (24)$$

Analyzing Eqs. (23) and (24), we can find a fact that $\frac{I_{zz}}{I_{xx}}$ only depends on ρ , n , $(\alpha_1 - \beta_1)$, and $(\alpha_2 - \beta_2)$ while $\frac{I_{zz}}{m}$ depends on ρ and the parameters of the group 1. Therefore, the derived close-form expressions describe strictly the relationship between the structure parameters and the mass geometry characteristics. That is, if given a payload, a configuration can be directly determined. When $\alpha_2 - \beta_2 = -(\alpha_1 - \beta_1)$, $r_{a1} = r_{a2}$, and $r_{b1} = r_{b2}$, the configuration is a standard Gough–Stewart parallel manipulator. Obviously, $I_{zz} = 4I_{xx} = 4I_{yy}$ exists substituting the relations in Eq. (24).

Theorem 2: A GSGSPM is easier to achieve dynamic isotropy than a standard Gough–Stewart parallel manipulator, even to remove the strict constraint $I_{zz} = 4I_{xx} = 4I_{yy}$. The compliance center of a GSGSPM can be also changed on a larger scale.

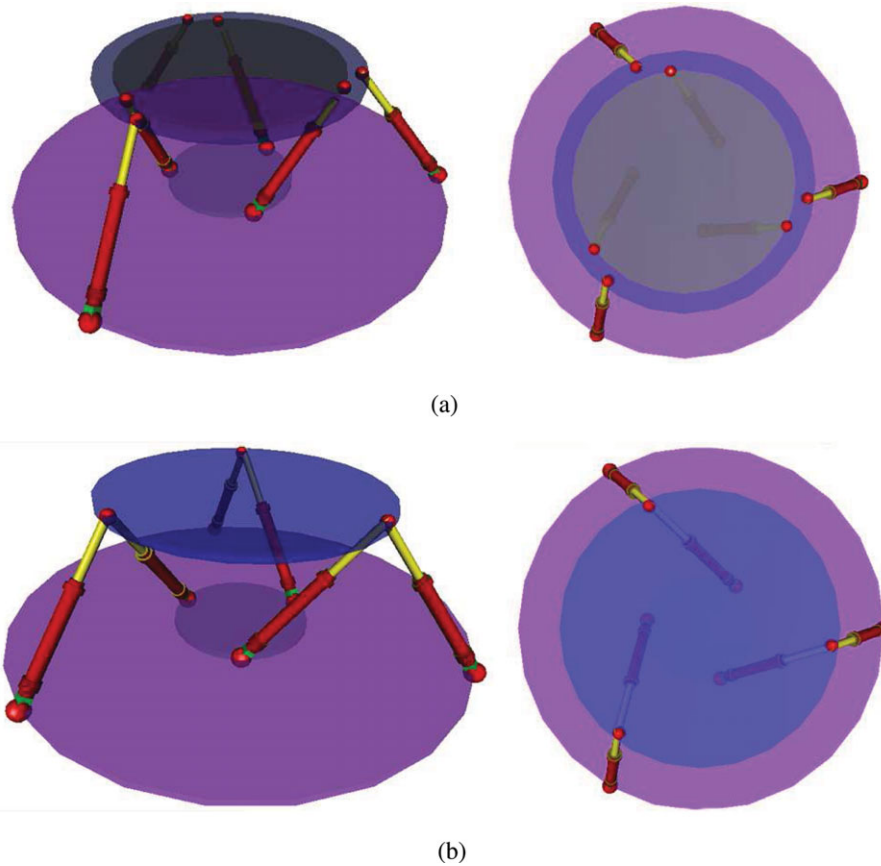


Fig. 2. (Colour online) The isotropic GSGSPMs: (a) 2C–2C GSGSPMs with $\rho \neq 1$; (b) 1C–2C GSGSPMs with $n = 1$ and $\rho = 1$.

Proof 1: Exacting a special case with $(\alpha_1 - \beta_1) = -(\alpha_2 - \beta_2)$ and $\frac{p}{q} = \frac{\rho^2 \sin(\alpha_1 - \beta_1)}{-n^2 \sin(\alpha_2 - \beta_2)} = 1$, then $\rho = n$. Substituting them in Eq. (24), we can obtain

$$\frac{I_{zz}}{I_{xx}} = \frac{(1 + \rho^2)^2}{\rho^2}. \tag{25}$$

Eq. (25) shows that $\frac{I_{zz}}{I_{xx}}$ is a function with minimum value. When $\rho = 1$, $(\frac{I_{zz}}{I_{xx}})_{\min} = 4$. When $\rho < 1$ or $\rho > 1$, then $I_{zz} > 4I_{xx}$ and $I_{zz} > 4I_{yy}$. Therefore, we can deduce that a GSGSPM can remove the strict constraint $I_{zz} = 4I_{xx} = 4I_{yy}$ when achieving complete isotropy than a standard Gough–Stewart parallel manipulator. Similarly, it can be proven that it is reachable that $I_{zz} < 4I_{yy}$. Therefore, the compliance center of a GSGSPM can be also changed on a larger scale.

Remark: If a standard Gough–Stewart parallel manipulator is expected to achieve complete dynamic isotropy, $I_{zz} = 4I_{xx} = 4I_{yy}$ must be met. In practice, it is hardly to be realized because of the strictly physical restriction. However, it is mechanical and feasible for a GSGSPM. Unfortunately, $I_{xx} = I_{yy}$ is a necessary restriction so that to satisfy complete isotropy of rotational motions. However, it is easier to assure $I_{xx} = I_{yy}$ in engineering applications.

4. Optimal Design of a Class of GSGSPMs with Dynamic Isotropy

4.1. Type synthesis

On the basis of the derived mathematical descriptions, a class of complete dynamic isotropic GSGSPMs can be

synthesized. According to numbers of circles on the movable platform and the fixed base, we can categorize GSGSPMs into three families, denoted by $iC-jC$. For example, 2C–2C GSGSPMs represent two circles on the movable platform and two ones on the fixed base.

- **Family 1: 2C–2C GSGSPMs**
GSGSPMs with a configuration $n = \frac{r_{a1}}{r_{a2}} \neq 1$ and $\frac{q}{n^2 p} = \frac{r_{b1}}{r_{b2}} \neq 1$ are called as 2C–2C GSGSPMs. According to the value of ρ , we categorize the geometry in two classes, including $\rho = 1$ and $\rho \neq 1$.

If $\rho = 1$, Eq. (24) is given by

$$\frac{I_{zz}}{I_{xx}} = \frac{16}{n^2} \times \frac{\sin^2(\alpha_1 - \beta_1)}{1 + \left(\frac{\sin(\alpha_1 - \beta_1)}{-n^2 \sin(\alpha_2 - \beta_2)}\right)^2 - 2 \left(\frac{\sin(\alpha_1 - \beta_1)}{-n^2 \sin(\alpha_2 - \beta_2)}\right) \cos((\alpha_1 - \beta_1) - (\alpha_2 - \beta_2))}. \tag{26}$$

By choosing the design variables, we can get complete dynamic isotropic GSGSPMs, as shown in Fig. 2(a), similar to the manipulators designed by Yi *et al.* It is a kind of the class dynamic isotropic GSGSPMs with $\frac{\sin(\alpha_1 - \beta_1)}{-\sin(\alpha_2 - \beta_2)} = \frac{r_{a2} r_{b2}}{\rho^2 r_{a1} r_{b1}}$ and $\rho \neq 1$.

- **Family 2: 1C–2C GSGSPMs**
This family requires either $n = \frac{r_{a1}}{r_{a2}} = 1$ or $\frac{q}{n^2 p} = \frac{r_{b1}}{r_{b2}} = 1$, that is, the family of 1C–2C GSGSPMs and the family of 2C–1C GSGSPMs are in equipollence. Each family of them can be also categorize the geometry in two classes, including $\rho = 1$ and $\rho \neq 1$.

If $n = 1$ and $\frac{q}{n^2 p} = \frac{r_{b1}}{r_{b2}} \neq 1$ and $\rho = 1$, it is a class of the family of 1C–2C GSGSPMs. Eq. (24) is given by

$$\frac{I_{zz}}{I_{xx}} = \frac{16 \sin^2(\alpha_1 - \beta_1)}{1 + \left(\frac{\sin(\alpha_1 - \beta_1)}{-\sin(\alpha_2 - \beta_2)}\right)^2 - 2\left(\frac{\sin(\alpha_1 - \beta_1)}{-\sin(\alpha_2 - \beta_2)}\right) \cos((\alpha_1 - \beta_1) - (\alpha_2 - \beta_2))} \quad (27)$$

If $n \neq 1$ and $\frac{q}{np} = \frac{r_{b1}}{r_{b2}} = 1$ and $\rho = 1$, it is a class of the family of 2C–1C GSGSPMs. Substituting in to Eq. (27) yields

$$\frac{I_{zz}}{I_{xx}} = \frac{16 \sin^2(\alpha_1 - \beta_1)}{1 + n^2 - 2n \cos((\alpha_1 - \beta_1) - (\alpha_2 - \beta_2))} \quad (28)$$

Fig. 2(b) is a kind of 1C–2C GSGSPMs with $n = 1$ ($r_{a1} = r_{a2}$) and $\rho = 1$ ($L_1 = L_2$). Therefore, $\frac{\sin(\alpha_1 - \beta_1)}{-\sin(\alpha_2 - \beta_2)} = \frac{r_{b1}}{r_{b1}}$.

• **Family 3: 1C–1C GSGSPMs**

A Gough–Stewart parallel manipulator with rotational symmetric geometry belongs to this family, that is, the strut lengths are not all equal but alternate equal. Therefore, the conditions are $n = \frac{r_{a1}}{r_{a2}} = 1$, $\frac{q}{np} = \frac{r_{b1}}{r_{b2}} = 1$, and $\rho \neq 1$. It implies that this family only includes one class. $\frac{\sin(\alpha_1 - \beta_1)}{-\sin(\alpha_2 - \beta_2)} = \frac{1}{\rho^2}$, and $\frac{I_{zz}}{I_{xx}}$ can be described as

$$\frac{I_{zz}}{I_{xx}} = 2(1 + \rho^2)^2 \frac{\sin^2(\alpha_1 - \beta_1)}{1 - \cos((\alpha_1 - \beta_1) - (\alpha_2 - \beta_2))} \quad (29)$$

4.2. *Optimal design approach*

The derived analytical formulations could be used to give a new optimal design of a GSGSPM. The structure parameters of a GSGSPM involve the layout angles of struts $\alpha_1 - \beta_1$ and $\alpha_2 - \beta_2$, the size of the fixed base platform r_{b1} and several dimensionless parameters, including ρ , p , q , and n . To ensure a feasible mechanism with compact structure, the design variables should be limited within the spaces of $0^\circ < \alpha_1 - \beta_1 \leq 120^\circ$, $0^\circ < \alpha_2 - \beta_2 \leq 120^\circ$, $r_{b1_{min}} \leq r_{b1} \leq \kappa r_{b1_{max}}$, $\rho_{min} \leq \rho \leq \rho_{max}$, $0 < p \leq 5$, $0 \leq q \leq 5$, and $0 \leq n \leq 1$, respectively. Because $r_{b1} \leq r_{b2}$, $\frac{q}{np} \leq 1$. The optimization problem can be described as follows:

- Objective function: Eqs. (23) and (24) are satisfied as possible.
- Optimal variables: $\alpha_1 - \beta_1$, $\alpha_2 - \beta_2$, r_{b1} , ρ , p , q , and n . Note that the number of free variables is different for each class and any one of $\alpha_1 - \beta_1$, $\alpha_2 - \beta_2$, ρ , p , q , and n can be calculated by the others.
- Subject to: $0^\circ < \alpha_1 - \beta_1 \leq 120^\circ$, $0^\circ < \alpha_2 - \beta_2 \leq 120^\circ$, $r_{b1_{min}} \leq r_{b1} \leq r_{b1_{max}}$, $\rho_{min} \leq \rho \leq \rho_{max}$, $0 < p \leq 5$, $0 \leq q \leq 5$, $0 \leq n \leq 1$, and $\frac{q}{np} \leq 1$.

The iterative design procedures are listed as follows:

- (a) Choose a family that is suitable for practical application.

- (b) For the payload’s center of mass criteria and inertial parameters, considering other constraints to determine r_{b1} , ρ , p , q , n , $\alpha_1 - \beta_1$, and $\alpha_2 - \beta_2$.

An optimal design can determine a solution by defining a cost function weighted by free parameters. It is favored in the robotics literature. However, for 1C–1C family, the number of free parameters is four including r_{b1} , $\alpha_1 - \beta_1$, $\alpha_2 - \beta_2$, and p , and the number of governing equations is five. It is impossible to satisfy the inertial parameters and the given compliance center if they come into opposition.

- (c) According to the requirements of isotropy conditions, calculate H_{ISO} .
- (d) To meet the task requirements, for example, dexterity, singularity and workspace, it is unavoidable to verify whether satisfy other performance measures. Further, it is necessary to ensure the mechanical feasibility, including the intersections among components. In mathematics, the intersections among components can be verified by calculating the angles between the unit vector of the struts and the axes of the joints. We have developed an environment of motion visualization to verify that configuration is mechanically valid. If some modifications are needed, return to step (b), and then, start next iteration.

This design is a multiple objectives and constrained optimization problem. It can be solved via a direct search method, such as the well-known Nelder-Mead simplex algorithm. However, this traditional routine heavily depends on good starting points. On the other hand, as a global method based on natural evolution, the genetic algorithm (GA) can be applied to solve a variety of optimization problems. The PSO, proposed by Kennedy and Eberhart²³, is a population-based stochastic optimization method inspired by the social behavior of swarm intelligence. PSO searches for optima by exploiting a population of potential solutions and probing the search space. PSO exchanges information between individuals, called particles, of the population, called swarm. Each particle adjusts its direction toward its own best position and toward the best previous position encountered by any other particles in the search space, which converges in optimal region of the searching. Compared to the GA, the PSO has no evolutionary operators in terms of crossover and mutation, and from the viewpoint of programming, the advantages of PSO are easy implementation and fewer adjustable parameters. The PSO costs a longer calculation time and possesses a better convergence rate than the GA procedure.²² In our optimization procedure, the mechanical feasibility of the obtained configuration is more important for real applications in condition that a longer computational time is available. Therefore, we prefer to use the PSO approach.

In the PSO, regarding a D -dimensional search space and a swarm consisting of N particles, the i th particle is represented by a D -dimensional vector $\mathbf{X}_i = (x_{i1}, x_{i1}, \dots, x_{iD})$, the velocity of this particle is $\mathbf{V}_i = (v_{i1}, v_{i1}, \dots, v_{iD})$, and the best position is recorded and represented as $\mathbf{P}_i = (p_{i1}, p_{i1}, \dots, p_{iD})$, which corresponds to a set of the optimal variables. For GSGSPMs optimization, the max dimensions

of the optimization problem are 6, 5, and 5 for three families, respectively. The particles are manipulated according to the following equations (the superscripts denote the iteration):

$$\mathbf{V}_i^{j+1} = w\mathbf{V}_i^j + c_1r_1[\mathbf{P}_i^j - \mathbf{X}_i^j] + c_2r_2[\mathbf{P}_g^j - \mathbf{X}_i^j], \quad (30)$$

$$\mathbf{X}_i^{j+1} = \mathbf{X}_i^j + \mathbf{V}_i^{j+1}, \quad (31)$$

where w is the inertia weight, c_1 and c_2 are positive constants called the cognitive and social parameters, respectively, r_1 and r_2 are random numbers uniformly distributed between 0 and 1. PSO technique has proven to be efficient for unconstrained and constrained optimization problems and easy implementation. In this paper, it is employed for the optimization of GSGSPMs.

Factually, the optimized manipulators are developed by a local dynamic isotropic measure. The obtained designs, however, might have worse dexterity, smaller workspace, or singular points among the reachable workspace. From a view of practice, passive joint limits and link interactions must be considered. These evaluations belong to global measures. Therefore, a grid-scanning process via numerical algorithm should be employed.

4.3. Examples and discussions on optimization results

In flight simulation, it is necessary to decouple motions and ensure the bandwidth uniform in order to replicate the given motions and provide the pilots motion cueing. Hence, it is an optimal design with dynamic isotropy. We use the payload inertial parameters of the Delft SIMONA motion system (configuration C) referring literature,²³ $\rho_c = [0 \ 0 \ 0.45]^T \text{m}$, $m = 4300 \text{ Kg}$, $\mathbf{I}_c = \text{diag}(4100, 4000, 6700) \text{ Kg}\cdot\text{m}^2$. Clearly, it is impossible to achieve complete isotropy because of $I_{xx} \neq I_{yy}$. Therefore, η_2 is equal to 1.025 using our algorithm, better than standard Gough–Stewart parallel manipulators extensively applied in flight simulation. We choose family 1 and family 2 to find solution due to their feasibility.

Considering the requirements of mounting space and workspace, additional constraints are introduced, including $H > 1.5 \text{ m}$ and $r_{b1} > 3 \text{ m}$ or $r_{b2} > 3 \text{ m}$. In PSO, the population size is assigned as 30 and the maximum generation number is set to 500. The acceleration constants are set to $c_1 = 1.2$ and $c_2 = 1.2$, respectively. In addition, the initial and final values of inertia weight are assigned as 0.8 and 0.2, respectively. If N is set to a greater number, the computational time will be longer while the convergence values will change a little between two neighboring. As far as the termination criterions should be proposed for the optimization procedure, one criterion is the maximum number of iterations without change (10), and another one is the termination tolerances (1.0E-6). The evolutions of behavioral variables are shown in Fig. 3, including three configurations.

The optimizations are convergent as listed in Tables I and II.

In view of the optimized results in Table II, we can observe that the configuration No. 3 has too large size to implement mechanically. Compared the configurations No.

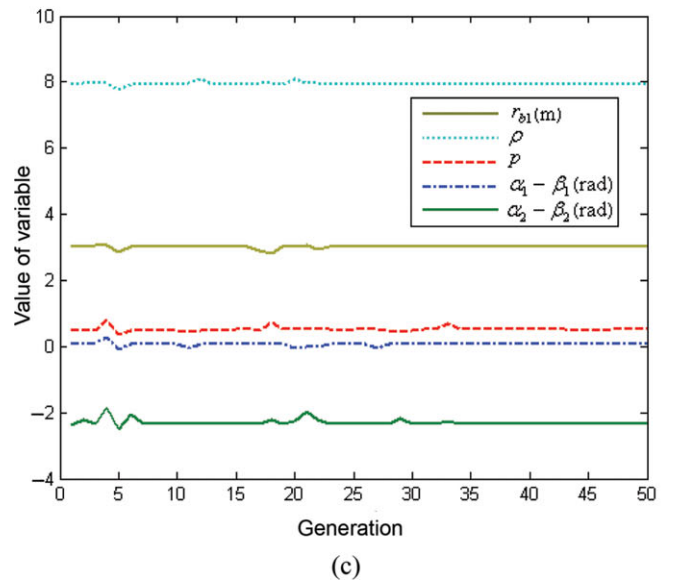
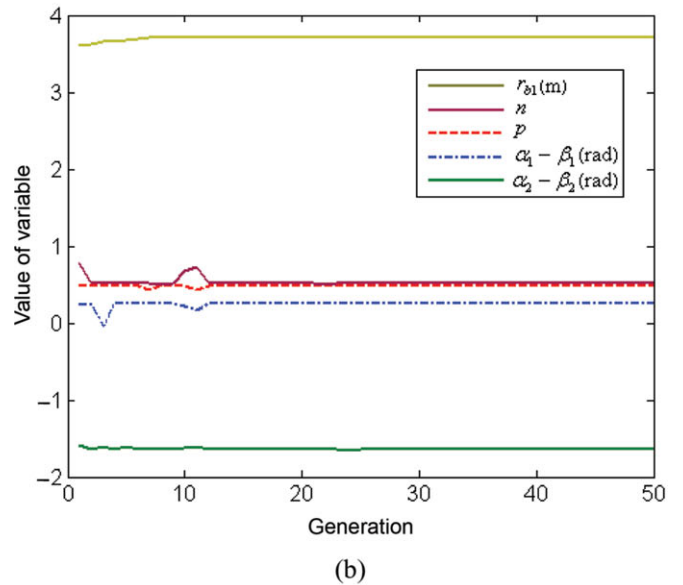
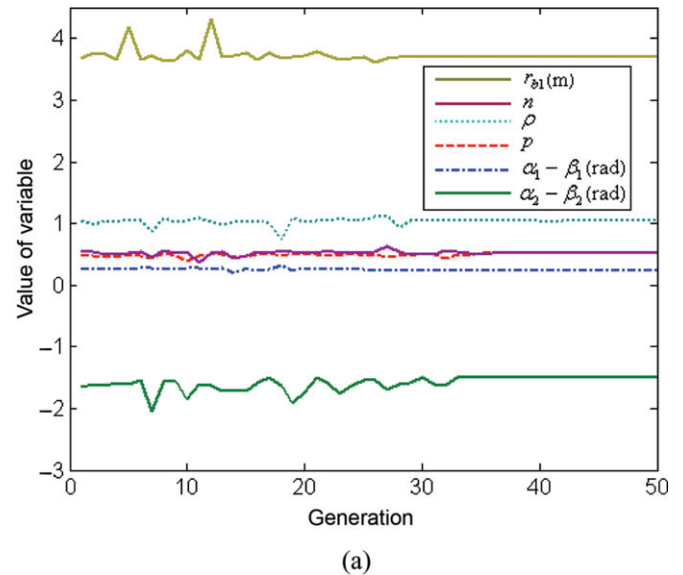


Fig. 3. (Colour online) The evolutions of behavioral variables of (a) configurations No. 1, (b) configurations No. 2, and (c) configurations No. 3.

Table I. Optimized results form PSO.

No.	$\alpha_1 - \beta_1 [^\circ]$	$\alpha_2 - \beta_2 [^\circ]$	r_{b1} (m)	ρ	p	q	n	Family type
1	13.9515	-86.3218	3.7090	1.0352	0.5092	0.5334	0.5208	2C–2C
2	14.6276	-88.9803	3.7052	1	0.4817	0.4998	0.5119	2C–2C
3	4.0844	-135.0049	3.0168	7.9397	0.5040	0.0794	1	1C–2C

Table II. Structure parameters of the optimized configurations.

No.	$\alpha_1 [^\circ]$	$\beta_1 [^\circ]$	$\alpha_2 [^\circ]$	$\beta_2 [^\circ]$	r_{a1} (m)	r_{b1} (m)	r_{a2} (m)	r_{b2} (m)	L_1 (m)	L_2 (m)	H (m)
1	15.3467	1.39515	-86.3218	0	1.8886	3.7090	0.9835	1.8439	2.3852	2.4691	1.4007
2	16.0904	1.46276	-88.9803	0	1.9140	3.7052	0.9798	1.9605	2.6648	2.6650	1.5385
3	4.0844	0	-135.0	0	1.5205	3.0168	1.5205	19.1584	2.5654	20.3685	2.0782

1 and No. 2, the later is preferable because its struts are all uniform and realized easily for structure design and control system. In addition, the obtained designs should be check whether worse dexterity, smaller workspace, singular points, or link interactions among the reachable workspace exist. Therefore, we evaluate these performances via numerical algorithm. In general case, a reachable workspace is a better comparison index. For simplicity, all the workspace graphs are determined by the constant orientation of the movable platform with no rotations. In order to evaluate dexterity in the global workspace, the condition number of the Jacobian, $\kappa = \|\mathbf{J}\|\|\mathbf{J}^{-1}\|$, is also calculated via numerical solution. The obtained results of three configurations are given in Figs. 4–6, respectively.

Generally, three optimized results all satisfy the specifications. The third geometry is worse than the first and the second due to higher position, worse kinematic symmetry, and dexterity. The second geometry is more mechanically

feasible than the first because its struts in two groups are all with the same length. This design example shows that an optimal routine could be realized based on the dynamic isotropy measure. Through a GGSPM is more complicate than a standard Gough–Stewart parallel manipulator, it can achieve almost the same performances as the latter and is more flexible due to the loosened physical restriction for the payload.

5. Conclusion

In this paper, we propose the concept of dynamic isotropy and used it as an optimum measurement to bridge the structure design and the control system design. The decoupled conditions and dynamic isotropy conditions are discussed and expressed analytically in close form without time-consuming numerical solution. The analytical formulations can be used to design dynamic isotropic GSGSPMs and be expected to help the designers in improving the dexterity

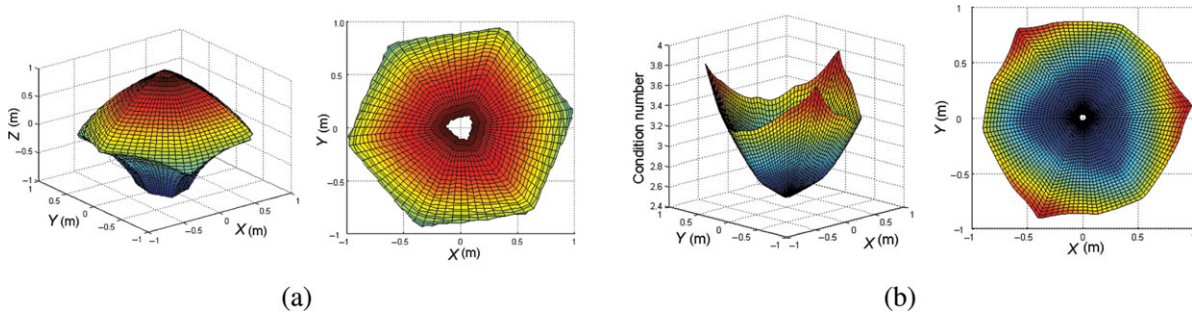


Fig. 4. (Colour online) 2C–2C configuration with $\rho \neq 1$: (a) reachable workspace shape; (b) condition number distribution.

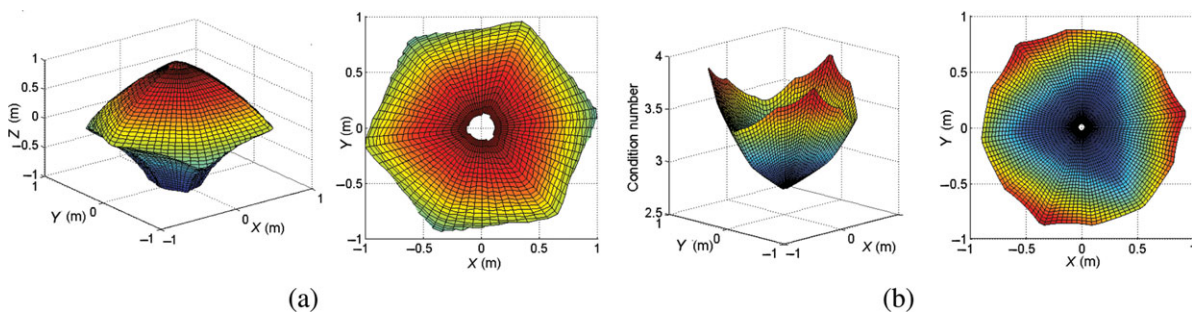


Fig. 5. (Colour online) 2C–2C configuration with $\rho = 1$: (a) reachable workspace shape; (b) condition number distribution.

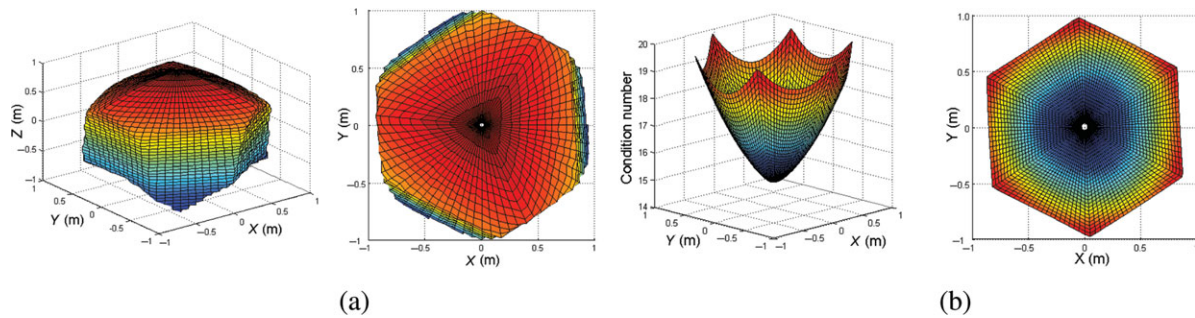


Fig. 6. (Colour online) 1C–2C configuration with $\rho \neq 1$: (a) reachable workspace shape; (b) condition number distribution.

of GSGSPMs. Furthermore, we present an optimal design routine based on PSO, which evaluates and verifies dexterity, singularity-free workspace, and mechanical feasibility to meet the special requirements.

Compared to the previous work, dynamic isotropy is more reasonable and systematical, which considers the relationships between geometry of the manipulator, mass-center and inertia parameters of the payload, and the response of the control system. All expressions are analytical and natural. What is more, we have found that a GSGSPM is easier to achieve isotropy than a standard Gough–Stewart parallel manipulator. It is significant for some special tasks requiring high precision and better dexterity, including laser weapon pointing and scanning microscopes.

Our future work includes investigating and extending this routine to more general parallel manipulators, for example, unsymmetrical parallel manipulators.

Acknowledgments

The authors appreciate the fund support from the Natural Science Foundation of China No. 50975055. The authors would like to thank the Project Supported by Development Program for Outstanding Young Teachers in Harbin Institute of Technology No. HITQNJ.S.2009.010.

References

1. J. P. Merlet, *Parallel Robots* (Kluwer Academic Publishers, Netherlands, 2000).
2. K. Y. Tsai and T. K. Lee, “6-DOF parallel manipulators with better dexterity, rotatability, or singularity-free workspace,” *Robotica* **27**, 599–606 (2009).
3. A. Fattah and A. M. H. Ghasemi, “Isotropic design of spatial parallel manipulators,” *Int. J. Rob. Res.* **21**, 811–824 (2002).
4. Y. X. Su, B.Y. Duan and C. H. Zheng, “Genetic design of kinematically optimal fine tuning Stewart platform for large spherical radio telescope,” *Mechatronics* **11**, 821–835 (2001).
5. S. Bandyopadhyay and A. Ghosal, “An algebraic formulation of kinematic isotropy and design of isotropic 6–6 Stewart platform manipulators,” *Mech. Mach. Theory* **43**, 591–616 (2008).
6. S. Bandyopadhyay and A. Ghosal, “An algebraic formulation of static isotropy and design of statically isotropic 6–6 Stewart platform manipulators,” *Mech. Mach. Theory* **44**, 1360–1370 (2009).
7. J. E. McInroy and J. Hamann, “Design and control of flexure jointed hexapods,” *IEEE Trans. Rob. Automat.* **16**(4), 372–381 (2000).
8. F. Jafari and J. E. McInroy, “Orthogonal Gough–Stewart platforms for micromanipulation,” *IEEE Trans. Rob. Automat.* **19**(4), 595–603 (2003).
9. Y. Yi, J. E. McInroy and F. Jafari, “Optimum Design of a Class of Fault-Tolerant Isotropic Gough–Stewart Platforms,” *Proceeding of the IEEE International Conference on Robotics and Automation*, New Orleans, LA (Apr. 2004) Vol. 5, pp. 4963–4968.
10. Y. Yi, J. E. McInroy and F. Jafari, “Generating Classes of Orthogonal Gough–Stewart Platforms,” *Proceeding of the IEEE International Conference on Robotics and Automation*, New Orleans, LA (Apr. 2004) Vol. 5, pp. 4969–4974.
11. Y. Yi, J. E. McInroy and F. Jafari, “Generating classes of locally orthogonal Gough–Stewart platforms,” *IEEE Trans. Rob. Automat.* **21**(5), 812–820 (2005).
12. K.Y. Tsai and K. D. Huang, “The design of isotropic 6-DOF parallel manipulators using isotropy generators,” *Mech. Mach. Theory* **38**(11), 1199–1214 (2003).
13. K. Y. Tsai and Z. W. Wang, “The design of redundant isotropic manipulators with special parameters,” *Robotica* **23**, 231–237 (2005).
14. K. Y. Tsai and T. K. Lee, “6-DOF Isotropic Parallel Manipulator with Three PPSR or PRPS Chains,” *Proceedings of the 12th IFToMM Conference*, Besancon, France (Jun. 2007) pp. 18–21.
15. K. Y. Tsai and S. R. Zhou, “The optimum design of 6-DOF isotropic parallel manipulators,” *J. Rob. Syst.* **22**(6), 333–340 (2005).
16. K. E. Zanganeh and J. Angeles, “Kinematic isotropy and the optimum design of parallel manipulators,” *Int. J. Rob. Res.* **16**(2), 185–197 (1997).
17. J. Angeles, “Is there a characteristic length of a rigid-body displacement?” *Mech. Mach. Theory* **41**, 884–896 (2006).
18. J. Hong-Zhou, H. E. Jing-Feng, T. Zhi-Zhong, “Characteristics analysis of joint space inverse mass matrix for the optimal design of a 6-DOF parallel manipulator,” *Mech. Mach. Theory* **45**(5), 722–739 (2010).
19. Y. Chen and J. E. McInroy, “Decoupled control of flexure-jointed hexapods using estimated joint-space mass-inertia matrix,” *IEEE Trans. Contr. Syst. Technol.* **12**(3), 413–421 (2004).
20. S. Bhattacharya, H. Hatwal and A. Ghosh, “On the optimum design of a Stewart platform type parallel manipulators,” *Robotica* **13**(2) 133–140 (1995).
21. J. Kennedy and R. C. Eberhart, “Particle Swarm Optimization,” *Proceedings of the IEEE International Conference on Neural Networks*, Perth, Australia (1995) pp. 1942–1948.
22. Q. Xu, Y. Li, “Error analysis and optimal design of a class of translational parallel kinematic machine using particle swarm optimization,” *Robotica* **27**, 67–78 (2009).
23. S. H. Koekebakker, *Model Based Control of a Flight Simulator Motion System Ph.D. Thesis* (Delft, Netherlands: Delft University of Technology, 2001).